Inorganic Chemistry
Article

Inorg. Chem. **2010**, *49*, 11249–11253 **11249**
DOI: 10.1021/ic1020912

Ligand Effects in Bimetallic High Oxidation State Palladium Systems

Alireza Ariafard,[†,‡] Christopher J. T. Hyland,[‡,§] Allan J. Canty,[*,‡] Manab Sharma,[‡] Nigel J. Brookes,[‡] and Brian F. Yates[*,‡]

[†]*Department of Chemistry, Faculty of Science, Central Tehran Branch, Islamic Azad University, Shahrak Gharb, Tehran, Iran,* [‡]*School of Chemistry, University of Tasmania, Private Bag 75, Hobart, Tasmania 7001, Australia, and* [§]*Department of Chemistry and Biochemistry, California State University, Fullerton, California 92831, United States*

Received October 15, 2010

Ligand effects in bimetallic high oxidation state systems containing a X−Pd−Pd−Y framework have been explored with density functional theory (DFT). The ligand X has a strong effect on the dissociation reaction of Y to form $[X-Pd-Pd]^+ + Y^-$. In the model system examined where Y is a weak σ-donor ligand and a good leaving group, we find that dissociation of Y is facilitated by greater σ-donor character of X relative to Y. We find that there is a linear correlation of the Pd−Y and Pd−Pd bond lengths with Pd−Y bond dissociation energy, and with the σ-donating ability of X. These results can be explained by the observation that the Pd d_{z^2} population in the PdY fragment increases as the donor ability of X increases. In these systems, the $Pd^{III}-Pd^{III}$ arrangement is favored when X is a weak σ-donor ligand, while the $Pd^{IV}-Pd^{II}$ arrangement is favored when X is a strong σ-donor ligand. Finally, we demonstrate that ligand exchange to form a bimetallic cationic species in which each Pd is six-coordinate should be feasible in a high polarity solvent.

Introduction

There is considerable current interest in developing a better understanding of mechanisms of catalytic reactions for formation of Ar^1-X and $N\sim Ar^1-Ar^2$ bonds involving palladium(II) acetate cyclopalladation of arenes containing a nitrogen donor ($N\sim Ar^1H$) in the presence of I^{III} oxidants such as $IPhX_2$[1] and $[IPhAr^2]BF_4$.[2] Recent reports[1c−g,2b] and commentary[3] are supportive of the intermediacy of binuclear species derived from oxidation of $[Pd^{II}(C\sim N)(\mu\text{-OAc})]_2$ (**1**) (Figure 1), in particular as a result of X-ray structural analyses of symmetrical $Pd^{III}-Pd^{III}$ species **2** (X = Y = Cl, C∼N = $\mathbf{L^1}$; X = Y = OAc, C∼N = $\mathbf{L^2}$) formed on application of $IPhCl_2$ and $IPh(OAc)_2$ as oxidants,[1b,d] and density functional theory (DFT) studies of reductive elimination from **2** with X = Y = Cl and C∼N = $\mathbf{L^1}$.[1f] In contrast, it is proposed

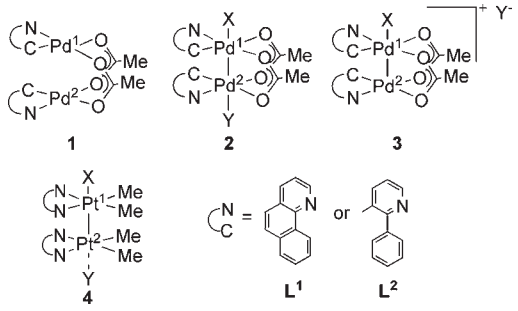

Figure 1. Potential geometries for bimetallic Pd and Pt species based on experimental observations.

that for $[IPh(Ar^2)]^+$ as oxidant, undetected species with configuration **3** (X = Ar^2, C∼N = $\mathbf{L^2}$) are formed,[1e,2b] on the basis of kinetic studies,[2b] and relationship to the platinum complex **4** (X = C≡CSiMe_3, Y = I, N∼N = 2,2′-bipyridine) characterized by X-ray crystallography;[4] preliminary DFT calculations suggest that the Pd···Pd interaction in **3** is minimal.[1e] The unsymmetrical complex **4** lacks bridging ligands, as also does a related symmetrical $Pt^{III}-Pt^{III}$ species characterized by X-ray crystallography and containing a N−Pt−Pt−N axis, $[PtCl(C\sim N)_2]_2$ (C∼N = 2-(pyridyl)-phenyl),[5] and these species provide an appreciation of the

*To whom correspondence should be addressed. E-mail: allan.canty@utas.edu.au (A.J.C.), brian.yates@utas.edu.au (B.F.Y.).

(1) (a) Dick, A. R.; Kampf, J. W.; Sanford, M. S. *J. Am. Chem. Soc.* **2005**, *127*, 12790. (b) Deprez, N. R.; Sanford, M. S. *Inorg. Chem.* **2007**, *46*, 1924. (c) Powers, D. C.; Ritter, T. *Nat. Chem.* **2009**, *1*, 302. (d) Powers, D. C.; Geibel, M. A. L.; Klein, J. E. M. N.; Ritter, T. *J. Am. Chem. Soc.* **2009**, *131*, 17050. (e) Lyons, T. W.; Sanford, M. S. *Chem. Rev.* **2010**, *110*, 1147. (f) Powers, D. C.; Benitez, D.; Tkatchouk, E.; Goddard, W. A., III; Ritter, T. *J. Am. Chem. Soc.* **2010**, *132*, 14092. (g) Powers, D. C.; Xiao, D. Y.; Geibel, M. A. L.; Ritter, T. *J. Am. Chem. Soc.* **2010**, *132*, 14530.

(2) (a) Kalyani, D.; Deprez, N. R.; Desai, L. V.; Sanford, M. S. *J. Am. Chem. Soc.* **2005**, *127*, 7330. (b) Deprez, N. R.; Sanford, M. S. *J. Am. Chem. Soc.* **2009**, *131*, 11234.

(3) (a) Hamilton, G. L.; Toste, F. D. *Nature* **2009**, *459*, 917. (b) Canty, A. J. *Dalton Trans.* **2009**, 10409.

(4) Canty, A. J.; Gardiner, M. G.; Jones, R. C.; Rodemann, T.; Sharma, M. *J. Am. Chem. Soc.* **2009**, *131*, 7236.

(5) Yamaguchi, T.; Kubota, O.; Ito, T. *Chem. Lett.* **2004**, *33*, 190.

Published on Web 11/02/2010

M···M interaction in the absence of ligands that may act to draw the metal atoms in close proximity independent of the extent of bonding. Extensive bridging has been observed in Pt^{III} species, for example, $[MePt(\mu\text{-pop-}P,P)_4PtI]^{4-}$ (pop^{2-} = $P_2O_5H_2^{2-}$) containing a Me−Pt−Pt−I axis related to **2**,[6] and amidate complexes such as $[Ph(H_3N)_2Pt(\mu\text{-O}\sim\text{N-}N,O)_2Pt(NH_3)_2]^{2+}$ ($O\sim N^-$ = $[O(HN)CBu^t]^-$) containing a Ph−Pt−Pt axis related to **3**.[7] A platinum analogue of **2** has also been recently reported, $[PtCl(C\sim N)(\mu\text{-OAc})]_2$ ($C\sim N$ = 2-(*p*-$EtOC_6H_3$)-5-(*p*-$EtOC_6H_4$)C_5H_3N), exhibiting the first example of liquid crystalline behavior for binuclear platinum dimers.[8]

Computational Details

Gaussian 09[9] was used to fully optimize all the structures reported in this paper at the M06[10] level of density functional theory. The choice of the M06 functional is based on the fact that this method is capable of considering the medium range $\pi-\pi$ stacking interactions in the bimetallic complexes and also of giving a reliable description of the relative energies in some transition-metal systems.[11] The effective core potential (ECP) of Hay and Wadt with a triple-ξ valence basis set (LANL2TZ) was chosen to describe Pd.[12] The 6-31G(d) basis set was used for other atoms.[13] A polarization function of $\xi_f = 1.472$ was also added to Pd.[14] This basis set combination will be referred to as BS1. Frequency calculations were carried out at the same level of theory as for structural optimization. To further refine the energies obtained from the M06/BS1 calculations, we carried out single point energy calculations for all the structures with a larger basis set (BS2). BS2 utilizes the quadruple-ζ valence def2-QZVP[15] basis set on Pd along with the corresponding ECP and the 6-311+G(2d,p) basis set on other atoms. The solvation energies were calculated using BS2 on gas phase optimized geometries with the CPCM solvation model[16] using dichloromethane and acetonitrile as solvents. To estimate the corresponding Gibbs free energies in solvents, ΔG, entropy corrections were calculated at the M06/BS1 level and added to the solvent potential energies. We have used the solvent energies throughout the paper unless otherwise stated. To further assess the relative energies derived from the M06 calculations, we also performed B97D[17]/BS2//M06/BS1 single point calculations in the two solvents CH_2Cl_2 and MeCN. The B97D calculations yield a similar result to the M06 calculations (see Table S1 in the Supporting Information). The natural population analyses (NPA) and natural bond orbital (NBO) analyses on the bimetallic complexes were performed in conjunction with BS3.[18] BS3 uses the valence-triple-ξ basis set LANL2TZ(f) along with the corresponding ECP on Pd and triple-ξ basis set 6-311G(d,p) on all remaining atoms. The AOMix program was also employed in conjunction with BS3 to compute the molecular orbital compositions.[19]

Table 1. Calculated ΔG_1 (kJ mol^{-1}) for eq *1* in CH_2Cl_2 and MeCN Using the M06/BS2//M06/BS1 Level of Theory

X	Y	ΔG_1 in CH_2Cl_2	ΔG_1 in MeCN
F	Cl	87.9	59.0
Cl	Cl	73.6	44.8
OC(O)Me	Cl	70.7	41.8
CN	Cl	53.1	23.8
C≡$CSiMe_3$	Cl	25.1	−1.7
C≡CH	Cl	22.6	−4.6
CF_3	Cl	14.2	−10.0
CH_2Ph	Cl	1.3	−23.0
Ph	Cl	1.3	−23.4
H	Cl	−0.8	−26.8
Me	Cl	−2.5	−27.6
C(O)Me	Cl	−9.6	−32.6
$SiMe_3$	Cl	−17.6	−40.2

Results and Discussion

The contrast between structures **2** and **3** suggests that the X group plays an important role in determining the geometry of these oxidation products. Herein, we use computational chemistry to investigate the influence of the X group on the geometry and lability of the bimetallic catalysis intermediates **2** and **3**. Initially we used the model reaction (eq 1),

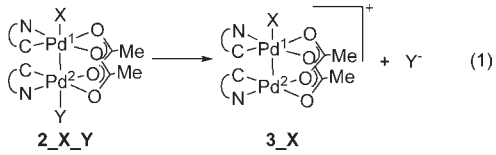

where complex **2_X_Y** dissociates to **3_X** + Y^-, keeping Y = Cl and using $\mathbf{L^1}$ in combination with a variety of X groups (Table 1). In the asymmetrical complexes **2_X_Cl**, the Cl group is a weak σ donor while the X groups vary from a weak σ donor such as F to a strong σ donor such as $SiMe_3$.

DFT was employed in conjunction with a low polarity solvent (CH_2Cl_2) and also a high polarity solvent (MeCN) in view of Sanford[1a,b,e,2] and Ritter's[1c,d] catalysis undertaken in highly polar media. The nature of the X group has a significant effect on determining which species, **2_X_Cl** or **3_X**, is the major intermediate. In general, the results (Table 1), which are ordered by ΔG_1, show that when X is a strong σ-donor ligand the Pd−Cl bond is weak and Cl^- dissociates more easily, rendering **3_X** the major intermediate. For example, when X = $SiMe_3$ reaction 1 has a negative value of ΔG_1 showing that the reaction is exergonic and thermodynamically favorable. On the other hand, when X is a weak σ-donor ligand, such as F, Cl, or OAc, reaction 1 is endergonic and **2_X_Cl** is the predominant intermediate.

The more polar solvent MeCN increases the level of Cl^- dissociation. For example, in CH_2Cl_2 when X = C≡CH or

(6) Che, C.-M.; Mak, T. C. W.; Gray, H. B. *Inorg. Chem.* **1984**, *23*, 4386.
(7) Ochiai, M.; Fukui, K.; Iwatsuki, S.; Ishihara, K.; Matsumoto, K. *Organometallics* **2005**, *24*, 5528.
(8) Santoro, A.; Wegrzyn, M.; Whitwood, A. C.; Donnio, B.; Bruce, D. W. *J. Am. Chem. Soc.* **2010**, *132*, 10689.
(9) Frisch, M. J. et al. *Gaussian 09*, revision A.02; Gaussian, Inc.: Wallingford, CT, 2009.
(10) (a) Zhao, Y.; Schultz, N. E.; Truhlar, D. G. *J. Chem. Theory Comput.* **2006**, *2*, 364. (b) Zhao, Y.; Truhlar, D. G. *J. Chem. Phys.* **2006**, *125*, 194101. (c) Zhao, Y.; Truhlar, D. G. *J. Phys. Chem. A* **2006**, *110*, 13126.
(11) (a) Sieffert, N.; Bühl, M. *Inorg. Chem.* **2009**, *48*, 4622. (b) Benitez, D.; Tkatchouk, E.; Goddard, W. A., III. *Organometallics* **2009**, *28*, 2643. (c) Benitez, D.; Shapiro, N. D.; Tkatchouk, E.; Wang, Y. M.; Goddard, W. A., III; Toste, F. D. *Nat. Chem.* **2009**, *1*, 482.
(12) (a) Hay, P. J.; Wadt, W. R. *J. Chem. Phys.* **1985**, *82*, 270. (b) Wadt, W. R.; Hay, P. J. *J. Chem. Phys.* **1985**, *82*, 284. (c) Roy, L. E.; Hay, P. J.; Martin, R. L. *J. Chem. Theory Comput.* **2008**, *4*, 1029.
(13) Hariharan, P. C.; Pople, J. A. *Theor. Chim. Acta* **1973**, *28*, 213.
(14) Ehlers, A. W.; Böhme, M.; Dapprich, S.; Gobbi, A.; Höllwarth, A.; Jonas, V.; Köhler, K. F.; Stegmann, R.; Veldkamp, A.; Frenking, G. *Chem. Phys. Lett.* **1993**, *208*, 111.
(15) Weigend, F.; Furche, F.; Ahlrichs, R. *J. Chem. Phys.* **2003**, *119*, 12753.
(16) Barone, V.; Cossi, M. *J. Phys. Chem. A* **1998**, *102*, 1995.
(17) (a) Grimme, S. *J. Comput. Chem.* **2004**, *25*, 1463. (b) Grimme, S. *J. Comput. Chem.* **2006**, *27*, 1787.
(18) Glendening, E. D.; Read, A. E.; Carpenter, J. E.; Weinhold, F. *NBO*, version 3.1; Gaussian, Inc.: Pittsburgh, PA, 2003.
(19) Gorelsky, S. I. *AOMix: Program for Molecular Orbital Analysis*; York University: Toronto, Canada, 1997; http://www.sf-chem.net/.

Table 2. Calculated Pd^2-Cl and Pd−Pd Bond Distances (Å), NBO Pd^2 d_{z^2} Orbital Populations[a], and NBO Charges on Cl in Bimetallic Complexes **2_X_Cl**

X	Pd^2-Cl	Pd^1-Pd^2	d_{z^2} population of Pd^2	NBO charges on Cl
F	2.449	2.626	1.568	−0.394
Cl	2.439	2.641	1.568	−0.372
OC(O)Me	2.440	2.639	1.564	−0.377
CN	2.470	2.659	1.610	−0.427
C≡CH	2.493	2.665	1.638	−0.468
C≡CSiMe$_3$	2.495	2.673	1.641	−0.470
CF_3	2.521	2.696	1.679	−0.508
CH_2Ph	2.537	2.725	1.714	−0.532
Ph	2.536	2.718	1.707	−0.536
H	2.532	2.704	1.706	−0.535
Me	2.543	2.710	1.717	−0.552
C(O)Me	2.558	2.745	1.742	−0.565
$SiMe_3$	2.572	2.766	1.777	−0.594

[a] With the Pd^1-Pd^2 bond as the *z*-axis.

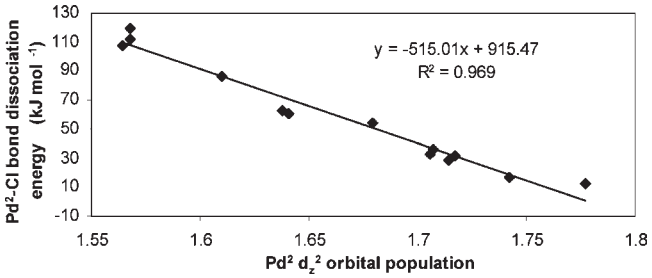

Figure 2. Relationship between calculated heterolytic bond dissociation energy for Pd^2-Cl and Pd^2 d_{z^2} orbital population.

CF_3, ΔG_1 is positive for reaction 1 but for MeCN ΔG_1 becomes negative favoring **3_X**. This can be assumed to result from stabilization of the charge separated species (**3_X** + Cl^-) by MeCN.

The Pd^2-Cl and Pd^1-Pd^2 bond lengths for the optimized structures **2_X_Cl** are presented in Table 2, and show that there is a linear correlation[20] of the Pd^2-Cl and Pd^1-Pd^2 bond lengths with the heterolytic Pd^2-Cl bond dissociation energies (Table 1) and with the σ-donating ability of X. Furthermore, as the σ-donating ability of X increases there is a corresponding increase in *both* the Pd^2-Cl and Pd^1-Pd^2 bond lengths. This latter observation can be explained by considering Natural Bond Orbital[18] (NBO) calculations which show that the d_{z^2} orbital population of the Pd^2 atom is increased when X is a strong σ-donor ligand. A plot of d_{z^2} orbital population of Pd^2 against Pd^2-Cl bond dissociation energy reveals a linear relationship (Figure 2). This result suggests that increasing the population of the d_{z^2} orbital leads to a greater propensity for Pd^2 to adopt a Pd^{II}-like arrangement. One of the contributing factors to this is that a higher d_{z^2} population results in increased repulsion between this orbital and a Cl lone-pair orbital, favoring dissociation of Cl^-. The shift in character toward a square planar geometry as the donor ability of X increases is further supported by the observed increase in Pd^1-Pd^2 bond length (Table 2).[21]

Given the strong dependency of the bimetallic intermediate on the identity of X, two bonding extremes can be envisaged,

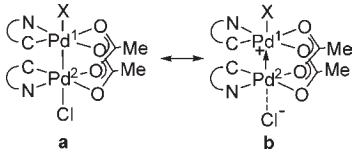

Figure 3. Proposed bonding extremes for **2_X_Cl**.

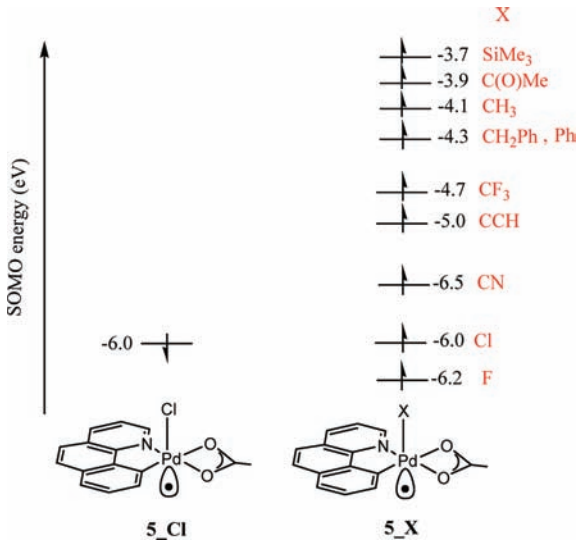

Figure 4. Diagram showing how the SOMO energy of **5_X** changes upon varying X, relative to the SOMO energy of **5_Cl**.

a and **b** in Figure 3. When X is a weak σ-donor ligand, such as F, Cl, or OAc, the $Pd^{III}-Pd^{III}$ structure **a** is likely to be the major contributor. Conversely, when X is a strong σ-donor ligand, such as $SiMe_3$, Me, or Ph, then the $Pd^{IV}-Pd^{II}$ structure **b** is a more dominant contributor. In our model structure **b**, chloride is largely dissociated as the anion and the formally positive Pd^{IV} center can be viewed as being stabilized to some extent by electron-donation from the d_{z^2} orbital of Pd^2. Additional support for this proposal is provided by the trend in increasing negative charge calculated for Cl as the σ-donating ability of X increases (Table 2).[22,23]

A molecular orbital analysis of the model systems **5_X** provides an estimate of the relationship between the singly occupied molecular orbital (SOMO) energy for Pd and the nature of the X group. This estimate can be used to relate the composition of the Pd−Pd bonding molecular orbital in the bimetallic species to the relative energies of the fragment molecular orbitals. Calculations with the model system **5_X** revealed that the energy level of the SOMO for Pd increases as the X group becomes a stronger σ-donor ligand (Figure 4).[24] When the SOMO energies for the Pd^1 and Pd^2 fragments are similar, then the Pd−Pd bond can be considered to be largely covalent. However, when the SOMO energy for Pd^1 rises, as is the case for strongly σ-donating X groups, the Pd−Pd bond becomes strongly polarized toward Pd^2. Spatial plots of the highest occupied molecular orbital (HOMO) in the bimetallic species can be constructed in terms of the bonding interaction

(20) See Figure S1 in the Supporting Information.

(21) The Pd−Pd bond length can also be affected by the trans influence of the ligands X and Y. Our calculation shows that, for example, the Pd−Pd bond length in **2_Ph_Ph** (2.773 Å) is noticeably longer than in **2_Cl_Cl** (2.641 Å). For further details see the Supporting Information.

(22) An excellent correlation (R^2 = 0.988) was obtained between the calculated Pd^2 d_{z^2} orbital population and the Cl NBO charge (Figure S3).

(23) No excellent correlation was observed between the Pd^2 d_{z^2} population and the Pd^1 and Pd^2 NBO charges (Figures S4 and S5).

(24) An excellent correlation (R^2 = 0.979) was obtained between the Pd^2 d_{z^2} orbital population and E_{SOMO}(**5_X**) − E_{SOMO}(**5_Cl**) (see the Supporting Information, Figure S2 for more details).

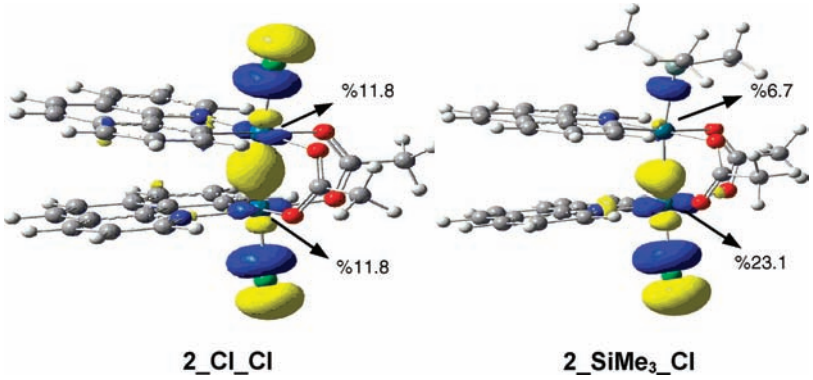

Figure 5. Resulting HOMO plot for **2_Cl_Cl** and **2_SiMe$_3$_Cl**.

Table 3. Calculated ΔG_1 (kJ mol^{-1}) for eq *1* with Variation of Y Using the M06/BS2//M06/BS1 Level of Theory

X	Y	ΔG_1 in CH_2Cl_2	ΔG_1 in MeCN
C≡CH	F	37.7	5.4
C≡CH	Cl	22.6	−4.6
C≡CH	Br	32.2	5.4
C≡CH	I	36.0	10.0
C≡CH	CN	49.0	21.8

of the Pd^1 and Pd^2 fragment SOMO orbitals. Figure 5 illustrates the HOMO for the two extreme cases of X = Cl and SiMe$_3$, respectively. As can be seen in these plots, the percent contribution[9] of the atomic orbitals of Pd^1 and Pd^2 to the HOMO is equal when X = Cl but is heavily weighted toward Pd^2 when X = SiMe$_3$. Overall, these analyses show that a strongly electron-releasing group on Pd^1 populates the d_{z^2} orbital of Pd^2, leading to more Pd^{II} character, resulting in dissociation of Y.

For the ethynyl group, which demonstrates behavior intermediate between F and SiMe$_3$ (Table 1), we have also explored the effect of variation of Y (Table 3). The calculations reveal that Pd^2−Y dissociation is very similar for Y = F, Cl, Br, and I, indicating that the identity of the halogen has little influence on Pd^2−Y dissociation. However, when Y is a stronger σ-donor such as CN, the Pd^2−Y interaction is increased, which is consistent with the general observation from Table 1.

We have probed the possibility that, upon dissociation of Y$^-$, coordination by solvent (MeCN) or another ligand (PMe$_3$) could occur at Pd^2 (eq 2).

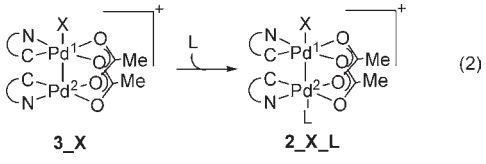

(2)

The calculated ΔG_2 for coordination of MeCN to the bimetallic species with varying X is positive, and thus thermodynamically unfavorable (Table 4). However, the likelihood of coordination of PMe$_3$ to Pd^2 in **3_X** was found to be dependent upon the nature of X, which is consistent with the discussion of eq 1 above. When X is a strong donor ligand, such as Ph, ΔG_2 is positive for association of PMe$_3$; when X is a weak donor, such as Cl, association of PMe$_3$ has a negative ΔG_2, indicating that formation of the phosphine complex **2_X_L** is favorable.

Table 4. Calculated ΔG_2 (kJ mol^{-1}) for eq *2* for L Binding to **3_X** with Variation of X Using the M06/BS2//M06/BS1 Level of Theory

X	L	ΔG_2 in CH_2Cl_2	ΔG_2 in MeCN
Cl	MeCN	18.0	20.9
C≡CH	MeCN	33.9	37.2
Ph	MeCN	35.1	38.1
Cl	PMe$_3$	−73.2	−76.1
C≡CH	PMe$_3$	−15.5	−14.2
Ph	PMe$_3$	12.1	16.3

Table 5. Calculated ΔG_3 (kJ mol^{-1}) for eq *3* in CH_2Cl_2 and MeCN Using the M06/BS2//M06/BS1 Level of Theory

X	Y	L	ΔG_3 in CH_2Cl_2	ΔG_3 in MeCN
Cl	Cl	PMe$_3$	0.4	−31.3
C≡CH	Cl	PMe$_3$	7.1	−18.8

As a possible guide for future synthetic chemistry, we have explored computationally the feasibility of replacing Y = Cl with Y = PMe$_3$ in **2_X_Y**, eq 3.

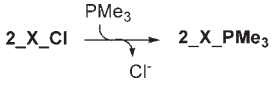

(3)

This is an important consideration given the frequent application of phosphine ligands in organometallic chemistry. It was found that, in the more polar solvent MeCN, substitution of Cl by PMe$_3$ is strongly favored ($\Delta G_3 < 0$), suggesting that more polar solvents would be suitable for the substitution of Y in **2_X_Y**, where X is a weaker donor ligand (Table 5). The more polar solvent favors this substitution because although the Pd−PMe$_3$ bond energy shows very little dependency upon solvent polarity, the dissociation of the Pd−Cl bond is favored in more polar solvents. In conclusion, substitution of Y in **2_X_Y** with a phosphine ligand is favored in the presence of a polar solvent for systems where X is a weak or moderate σ-donor.

Conclusions

The results presented here shed light on some of the differences in bonding in the bimetallic structures of the type discussed by Sanford and Ritter. Notably, for [X(C∼N)Pd^1-(μ-OAc)$_2$-Pd^2(C∼N)Y] we have demonstrated that increasing the population of the d_{z^2} orbital on Pd^2 by using a strong σ-donor X ligand causes a shift in bonding mode character from Pd^1(III)-Pd^2(III) toward Pd^1(IV)-Pd^2(II), facilitating

dissociation of Y^-. We believe that this information should assist in controlling the oxidation states of the metals and allow further optimization of this important class of catalyst systems. Our results also identify which bimetallic complexes are able to undergo displacement of chloride with neutral donor ligands such as PMe_3. This should be extendable to other neutral ligands and opens up the possibility of exploring new chemistry with the resulting cationic 6-coordinate systems.

Acknowledgment. We thank the Australian Research Council for financial support, and the Australian National Computational Infrastructure and the University of Tasmania for computing resources.

Supporting Information Available: Complete ref 9, linear correlations of data, additional information regarding the NBO calculation, Cartesian coordinates of all optimized structures. This material is available free of charge via the Internet at http://pubs.acs.org.

Note Added after ASAP Publication. This paper was published on the Web on November 2, 2010, with a minor text error in the Introduction section. The corrected version was reposted on November 5, 2010.